ACS Medicinal Chemistry Letters
Cite This: ACS Med. Chem. Lett. 2019, 10, 425−430
Letter
pubs.acs.org/acsmedchemlett

Inhibition of PCSK9^{D374Y}/LDLR Protein−Protein Interaction by Computationally Designed T9 Lupin Peptide

Carmen Lammi,[†] Jacopo Sgrignani,[‡] Gabriella Roda,[†] Anna Arnoldi,[†] and Giovanni Grazioso*,[†]

[†]Dipartimento di Scienze Farmaceutiche, Università degli Studi di Milano, Via L. Mangiagalli 25, 20133 Milan, Italy
[‡]Istituto di Ricerca in Biomedicina (IRB), Università della Svizzera Italiana (USI), Via V. Vela 6, CH-6500 Bellinzona, Switzerland

Supporting Information

ABSTRACT: The inhibition of the PCSK9/LDLR protein−protein interaction is a promising strategy for developing new hypocholesterolemic agents. Familial hypercholesterolemia is linked to specific PCSK9 mutations: the D374Y is the most potent gain-of-function (GOF) PCSK9 mutation among clinically relevant ones. Recently, a lupin peptide (T9) showed inhibitory effects on this mutant PCSK9 form, being also capable to increase liver uptake of low density lipoprotein cholesterol. In this Letter, aiming to improve the potency of this peptide, the T9 residues mainly responsible for the interaction with PCSK9^{D374Y} (hot spots) were computationally predicted. Then, the "non-hot" residues were suitably substituted by new amino acids capable to theoretically increase the structural complementarity between T9 and PCSK9^{D374Y}. The outcomes of this study were confirmed by *in vitro* biochemical assays and cellular investigations, showing that a new T9 analog is able to increase the LDLR expression on the liver cell surface by 84% at the concentration of 10 μM.

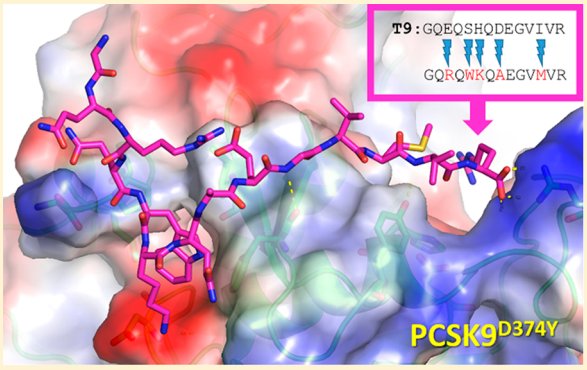

KEYWORDS: *Alanine scanning, HepG2 cells, PCSK9 inhibitors, MM-GBSA, LDL-R, bioactive peptides*

Proprotein convertase (PC) subtilisin/kexin type 9 (PCSK9) is a serine protease belonging to the PC family that is recognized as a key regulator of circulating low-density lipoprotein (LDL) cholesterol (LDL-c) since physiologically it binds to the LDL receptor (LDLR) and triggers its degradation into lysosomes.[1,2] In some pathological conditions (such as familiar hypercholesterolemia), PCSK9 displays enhanced LDLR affinity, and lowering the LDLR population on cell membrane leads to an increase of the circulating LDL-c levels. Consequently, impairing the PCSK9/LDLR interaction represents a strategy to increase the LDLR population on cell membrane and the consequent reduction of circulating LDL-c. For example, an effective clinical approach to interfere with the PCSK9/LDLR protein−protein (PPI) consists in the use of mAbs, such as *alirocumab* and *evolocumab*, approved for therapy by the American Food and Drug Administration in 2015.[3] Moreover, heparin sulfate-mimetics,[4] peptidomimetics,[5−7] or natural products, such as berberine,[8] have also demonstrated PCSK9 inhibitory activity, but at present, these approaches seem to be far from any clinical application. Recently, despite their known low oral bioavailability, innovative solutions for controlling their metabolism and advanced administration strategies[9−11] have renewed the interest for novel inhibitory peptides.[12−14] In this field, Zhang and co-workers have identified some peptides displaying PCSK9 inhibitory activity,[7,15] whereas we have identified a natural peptide from lupin proteins (LILPKHSDAD, P5), which inhibits PCSK9 in the low micromolar range.

Some PCSK9 mutants result in different physiological behaviors of PCSK9, and familiar hypercholesterolemia and additional research efforts are needed to inhibit them. Among them, the D374Y has been proven to be the most potent gain-of-function (GOF) PCSK9 mutation,[16,17] displaying a LDLR binding capacity 25 times greater than the wild type (WT) at the physiological 7.4 pH.[1,18] Interestingly, we have revealed that another lupin peptide (GQEQSHQDEGVIVR, T9) impairs the PCSK9^{D374Y}/LDLR interaction with an IC_{50} value of 286 μM,[19] whereas P5 is practically inactive.

In this Letter, aiming to improve the inhibitory effect of T9, an *in silico* procedure was applied in order to predict the binding mode of T9 and the residues mainly responsible for the interaction with PCSK9^{D374Y} (hot spots). Then, computational chemistry studies were carried out to identify substitutions of the "non-hot" residues able to increase the structural complementarity between T9 and PCSK9^{D374Y}. Finally, a novel T9 analog peptide was evaluated by

Special Issue: Highlighting Medicinal Chemistry in Italy

Received: October 5, 2018
Accepted: December 3, 2018
Published: December 3, 2018

DOI: 10.1021/acsmedchemlett.8b00464
ACS Med. Chem. Lett. 2019, 10, 425−430

biochemical assays and cellular investigations, displaying an improved biological activity.

RESULTS AND DISCUSSION

PCSK9^{D374Y}/T9 Complex Model. The geometry of the PCSK9^{D374Y}/T9 model was obtained by Ambertools16,[20] modifying the primary structure of the previously developed PCSK9^{WT}/T9 computational model.[5] MD simulations accomplished on the resultant model permitted the geometrical equilibration of the new residue in position 374 and permitted to exclude any ligand unbinding events (Figure S1 and Table S1, Supporting Information). Figure 1A displays the T9 binding mode before MD simulations, whereas, at the end of MD simulations, T9 was stabilized on PCSK9^{D374Y} by the following contacts (Figure 1B): (1) H-bonds by the side chains of Q2 and S5 with the one of D192; (2) H-bonds between the backbone of S5, H6, and E9 with the amide group of S376, Y374, and the side chain of Y374; (3) van der Waals contacts by the aliphatic chain of I12 with PCSK9^{D374Y} area shaped by residues C378, V380, and Y374; (4) van der Waals contacts by the side chain of V13 with A220; (5) H-bonds by the C-terminus of R14 with the side chains of Q382 and H226. Finally, the arginine group of R14 produced salt bridges with the negative charged area surrounded by E366 and D367. This binding mode was stably adopted by T9 after the first 100 ns of MD simulations (Figure 1C).

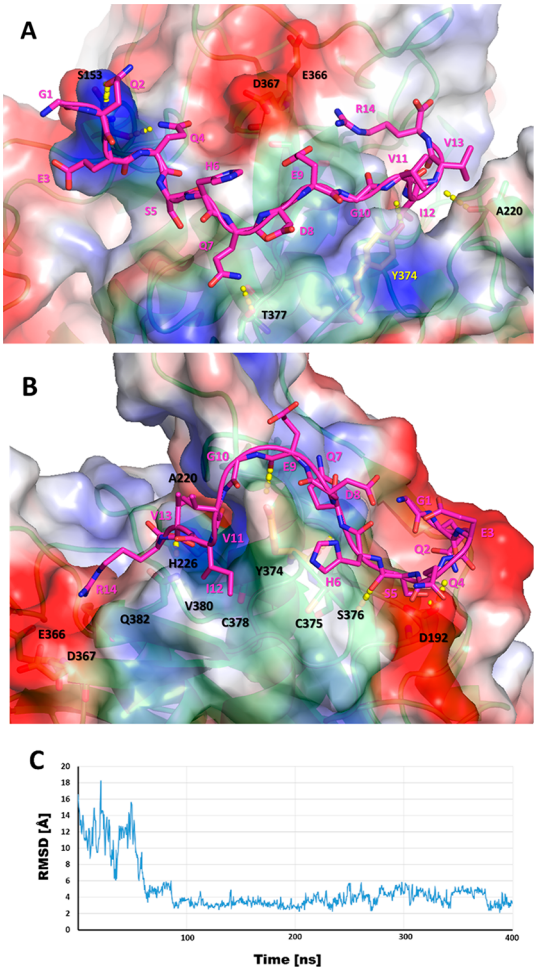

Figure 1. Expected T9 binding mode on PCSK9^{D374Y} surface, as resulted before (A) and after (B) MD simulations. Dotted yellow lines highlight the H-bond network, while the enzyme solvent accessible surface is depicted accordingly with the partial charge of the residues: blue for positive and red for negative areas, respectively. T9 is represented as magenta sticks. Panel C shows the RMSD plot of the T9 backbone atoms with respect to the peptide average structure. The complex backbone was previously aligned with respect to the initial minimized structure.

Identification of Hot Spots and Design of T9 Analogs. The first step in the rational design of peptide analogs is the identification of the role played by each residue in the template peptide. After recognition of the residues mainly contributing to the binding energy of the interacting peptides (hot spots), the "non-hot" residues are properly substituted by other amino acids, which may ensure a better complementarity between the biological counterparts. Here, the T9 hot and non-hot spots were identified by performing computational alanine-scanning mutagenesis analysis. Briefly, in the starting PCSK9^{D374Y}/T9 complex model,[19] each peptide residue was systematically mutated into alanine and the resulting complexes were then subjected to MD simulations. Therefore, MM-GBSA calculations were accomplished to obtain estimates of the mutant peptides binding free energy (ΔG^*, Table 1).[21,22] The data in Table 1 suggested that the T9 C-terminus seemed to be essential for the peptide binding since the substitution of the residues in positions 11, 13, and 14 by alanine led to peptides with estimated binding free energies significantly lower than the starting one.

Table 1. Estimated Binding Free Energy Values of the Peptides under Investigations, Calculated by MM-GBSA Approach (ΔG^*, Column 3)[a]

peptide	sequence	ΔG^* value [kcal/mol ± (std. err. of mean)]
T9	GQEQSHQDEGVIVR	−29.2 ± 0.8
T9D8A	GQEQSHQAEGVIVR	−45.1 ± 0.8
T9Q7A	GQEQSHADEGVIVR	−42.4 ± 1.0
T9I12A	GQEQSHQDEGVAVR	−41.7 ± 0.7
T9E9A	GQEQSHQDAGVIVR	−38.6 ± 1.0
T9H6A	GQEQSAQDEGVIVR	−38.5 ± 1.0
T9Q4A	GQEASHQDEGVIVR	−37.8 ± 0.6
T9G10A	GQEQSHQDEAVIVR	−37.1 ± 0.7
T9G1A	AQEQSHQDEGVIVR	−30.5 ± 0.8
T9S5A	GQEQAHQDEGVIVR	−29.4 ± 0.6
T9E3A	GQAQSHQDEGVIVR	−27.4 ± 0.6
T9Q2A	GAEQSHQDEGVIVR	−27.2 ± 0.8
T9V11A	GQEQSHQDEGAIVR	−25.4 ± 0.6
T9V13A	GQEQSHQDEGVIAR	−21.3 ± 0.8
T9R14A	GQEQSHQDEGVIVA	−19.7 ± 0.6

[a]Mutated peptides were sorted by calculated ΔG^* value.

However, our estimations also suggested that D8A mutation improved the binding affinity of the resulting peptide, whereas the side chain deletion of the residues in positions 6, 7, 9, and 12 was less effective in improving the peptide−enzyme complementarity. In other words, the original side chains in those positions do not seem to be well adapted to the PCSK9^{D374Y} counterpart since their substitution by a methyl group improved the affinity of the resulting peptides.

The preliminary biochemical evaluation of the T9D8A ability to impair the binding of the PCSK9^{D374Y} to its target LDLR was performed by *in vitro* experiments. Results indicated that T9D8A reduced the PCSK9-LDLR PPI by 31.3 ± 1.79%

DOI: 10.1021/acsmedchemlett.8b00464
ACS Med. Chem. Lett. 2019, 10, 425−430

Table 2. Estimated Binding Affinity Values of the New Designed Peptides (Columns 1, 2), Calculated by Prime Software (Δ Affinity, Column 3) and by Standard MD/MM-GBSA Calculations (ΔG* Values, Column 4)[a]

peptide name	mutation	sequence	Δ affinity [kcal/mol]	ΔG* value [kcal/mol ± (std. err. of mean)]
T9D8A	D8A	GQEQSHQAEGVIVR	0	−45.1 ± 0.8
T9D8A_A	H6K-D8A-I12M	GQEQSKQAEGVMVR	−14.1	−43.0 ± 0.8
T9D8A_B	H6R-D8A-E9M	GQEQSRQAMGVIVR	−14.0	−39.8 ± 0.8
T9D8A_C	H6R-Q7R-D8A	GQEQSRRAEGVIVR	−16.2	−37.4 ± 0.7
T9D8A_D	H6W-Q7R-D8A	GQEQSWRAEGVIVR	−13.2	−35.1 ± 0.6
T9D8A_E	H6F-Q7R-D8A	GQEQSFRAEGVIVR	−12.4	−34.2 ± 0.6
T9D8A_F	H6K-Q7R-D8A	GQEQSKRAEGVIVR	−14.4	−33.4 ± 0.8
T9D8A_G	H6P-Q7R-D8A	GQEQSPRAEGVIVR	−12.7	−31.0 ± 0.6
T9D8A_H	H6L-Q7R-D8A	GQEQSLRAEGVIVR	−12.3	−29.8 ± 0.6
T9D8A_J	H6R-Q7W-D8A	GQEQSRWAEGVIVR	−16.1	−27.6 ± 0.9
T9D8A_K	H6Y-Q7R-D8A	GQEQSYRAEGVIVR	−12.5	−24.0 ± 0.6

[a]See Supporting Information for details.

Table 3. Estimated Binding Affinity Values of the New Designed Peptides (Columns 1-2), Calculated by Prime Software (Δ Affinity, Column 3) and by Standard MD/MM-GBSA Calculations (ΔG* Values, Column 4)[a]

peptide name	mutation	sequence	Δ affinity [kcal/mol]	ΔG* value [kcal/mol ± (std. err. of mean)]
T9D8A_A	H6K-D8A-I12M	GQEQSKQAEGVMVR	0	−43.0 ± 0.8
T9D8A_1	E3R-S5W−H6K-D8A-I12M	GQRQWKQAEGVMVR	−28.9	−54.7 ± 1.0
T9D8A_2	E3W−S5W-H6K-D8A-I12M	GQWQWKQAEGVMVR	−25.2	−49.1 ± 0.6
T9D8A_3	E3I−S5W-H6K-D8A-I12M	GQIQWKQAEGVMVR	−25.7	−39.8 ± 1.4
T9D8A_4	E3T-S5W−H6K-D8A-I12M	GQTQWKQAEGVMVR	−25.1	−34.6 ± 0.6
T9D8A_5	E3R-S5F−H6K-D8A-I12M	GQRQFKQAEGVMVR	−22.9	−34.0 ± 0.9
T9D8A_6	E3R- H6K-Q7R-D8A-I12M	GQWQSKRAEGVMVR	−24.1	−31.1 ± 0.6
T9D8A_7	E3W−S5L-H6K-D8A-I12M	GQWQLKQAEGVMVR	−23.9	−29.9 ± 0.8
T9D8A_8	E3M-S5W−H6K-D8A-I12M	GQMQWKQAEGVMVR	−25.2	−29.4 ± 0.5
T9D8A_9	E3S−S5W-H6K-D8A-I12M	GQSQWKQAEGVMVR	−23.5	−28.6 ± 1.1
T9D8A_10	E3L-S5W−H6K-D8A-I12M	GQLQWKQAEGVMVR	−24.3	−19.0 ± 0.8

[a]See Supporting Information for details.

at the fixed concentration of 100 μM. However, T9D8A did not exhibit a clear dose−response profile, when it was tested in the concentration range of 0.1 μM to 1 mM (data not shown). Probably, the substitution of a negatively charged side chain (D) by a methyl group (A) altered the peptide folding and the overall physical−chemical properties.

As a consequence, it was hypothesized that the T9 primary structure could be additionally enhanced by the substitution of the amino acids in the "non-hot" positions. Accordingly, in a second step, 10,000 possible 6, 7, 9, and 12 T9D8A analogs were designed, and their affinity for PCSK9 were evaluated by the PRIME tool, implemented in the Schrödinger modeling suite. Only two simultaneous sequence mutations were accepted in those calculations to avoid huge alterations of the original peptide sequence. Finally, the complexes between PCSK9 and the top ranked peptide analogs (i.e., the ten showing the lowest Δ affinity values, Table 2) were submitted to MD simulations and their ΔG* values estimated by MM-GBSA calculations (Table 2).

Surprisingly, whereas by ΔΔG calculated by PRIME all analogs were hypothetically more active than T9, the majority of them showed MM-GBSA estimations not lower than peptide T9D8A (Table 2). These results were rationalized by the visual inspection of the MD simulations trajectories obtained simulating the T9D8A_A analog. Here, a conformational instability of the peptide *N*-terminal end was noted. Therefore, a second stage of PRIME calculations was accomplished, mutating the positions 3, 5, and 7. Once again, two simultaneous changes in the sequence were accepted in the PRIME calculations. The following MD simulations and MM-GBSA calculations on the ten top ranked $PCSK9^{D37Y}$/T9 analogs led to the results collected in Table 3. Here, the T9D8A_1 peptide acquired the lowest estimated binding free energy value by both approaches. Considerably, this peptide displayed the expected conformational stability, over more than 400 ns-long MD simulations (Figure S2, Supporting Information). The attained trajectory suggested that the novel T9 analog was firmly bound on the $PCSK9^{D374Y}$ surface (Figure 2) by (1) two H-bond/salt bridges by the C-terminus (R14) with the $PCSK9^{D374Y}$ R215 residue and by K6 with $PCSK9^{D374Y}$D238; (2) van der Waals contacts of the indole ring of W5 and the hydrophobic pocket sized by $PCSK9^{D374Y}$ F379, P156, and I369 residues; (3) a H-bond by the NH of M12 and the side chain of $PCSK9^{D374Y}$ Y374; (4) a H-bond by the NH of G10 and the backbone of $PCSK9^{D374Y}$F379; (5) the side chains of Q2 and Q4 with the $PCSK9^{D374Y}$ N-terminus (S153). Additionally, an internal salt bridge between the side chains of R3 and E9, strongly limited the conformational freedom of the novel peptide.

In agreement with these outcomes, peptide T9D8A_1 was synthesized by the GenScript Company and submitted to biochemical and cellular investigations.

Biochemical Evaluation of the T9D8A_1 Ability To Impair the $PCSK9^{D374Y}$-LDLR PPI. With the aim at evaluating the ability of the T9 analog to reduce the binding of $PCSK9^{D374Y}$ to its target LDLR, *in vitro* experiments were performed. More in detail, T9D8A_1 was tested in the concentrations range of 0.1 μM to 1 mM. Figure 3A indicates

DOI: 10.1021/acsmedchemlett.8b00464
ACS Med. Chem. Lett. 2019, 10, 425−430

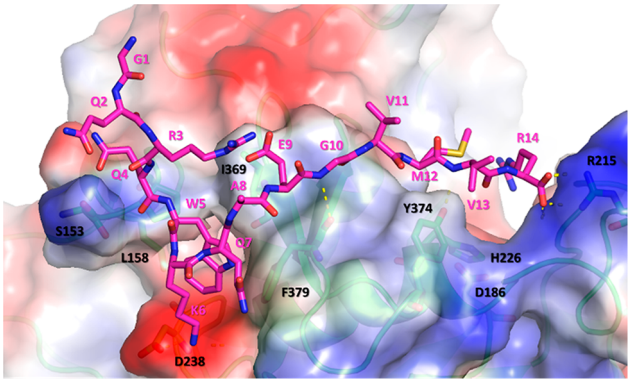

Figure 2. Expected binding mode of T9D8A_1 on PCSK9^{D374Y} surface, as resulted by docking and MD simulations. Dotted yellow lines depict the H-bond network. The enzyme solvent accessible surface is depicted according to the partial charge of the residues, blue for positive and red for negative areas.

that the T9 analog decreases the PPI in a concentration−response manner with an IC_{50} value of 147.8 ± 3.23 μM versus the untreated sample (Figure 3A).

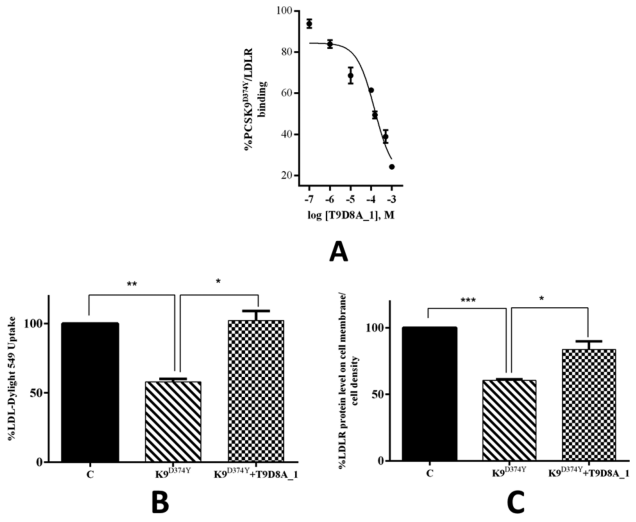

Figure 3. (A) Dose−response effects of peptide T9D8A_1 on the PPI between PCSK9 and the LDLR. Each point represents the average ± SD of three experiments in duplicate. T9D8A_1 peptide improves the ability of HepG2 cells to uptake extracellular LDL (B) due to an increase of the LDLR protein level located on the cell surfaces (C). Bars represent averages ± SD of three independent experiments in triplicates. (*) $p < 0.05$, (**) $p < 0.001$, and (***) $p < 0.0001$ versus control (C) and K9^{D374Y}/PCSK9^{D374Y}.

This value indicates that the computationally designed T9D8A_1 is twice more active than T9 in inhibiting the PCSK9^{D374Y}/LDLR PPI. In fact, recent results demonstrated that T9 inhibits this PPI by an IC_{50} value of 285.6 ± 2.46 μM.[19] Based on these *in vitro* results, further experiments were carried out to characterize in a deeper way the T9 analog ability to modulate the LDLR protein level and activity at cellular level.

T9D8A_1 Ameliorates the HepG2 Ability To Uptake LDL Increasing the LDLR Protein Level on the Cell Surface. After a 2 h treatment in the presence of PCSK9^{D374Y} (4.0 μg/mL), the ability of HepG2 cells to uptake the LDL-C from the extracellular environment was reduced by 42.1 ± 1.6% versus control, whereas the treatment with 10.0 μM T9D8A_1 totally re-establishes the uptake level up to 102.3 ± 4.8% versus the untreated sample (Figure 3B). This result strongly suggests that T9D8A_1 is 35-times more active than T9 from a functional point of view. In fact, when the parent peptide T9 was coincubated with the same concentration of GOF mutated PCSK9, it restored the uptake level of HepG2 cells only at the concentration of 350 μM.[19] This result suggests the potential involvement of an additional mechanism of action by which T9D8A_1, after permeation of HepG2 cells, might modulate other molecular targets involved in the cholesterol pathway. In fact, the potential ability of the parent peptide T9 to inhibit the HMGCoAR enzyme has been also predicted by computational study.[23] Of course, additional biological experiments are needed to confirm this hypothesis.

The functional results, which are in agreement with the *in vitro* findings, are linked to the ability of the T9 analog to modulate the LDLR protein activity on the hepatic cell surface. By performing in-cell western (ICW) experiments,[19,24] it was observed that, in the presence of PCSK9^{D374Y} (4.0 μg/mL), the LDLR protein levels on the HepG2 cell surface were diminished by 39.6 ± 0.7% versus the control cells and that T9D8A_1 (10 μM) restored the LDLR protein levels up to 83.8 ± 4.3% (Figure 3C). This is a clear evidence that the increased ability of hepatic cells to uptake the LDL-C from the extracellular environment in the presence of mutated PCSK9 after treatment with T9D8A_1 is correlated with the augmentation of the activity of the LDLR expressed on the cell surface. Moreover, this result confirms that T9D8A_1 is 35-times more active than T9, not only from a functional (in terms of HepG2 cell ability to uptake LDL from the extracellular level) but also from a molecular point of view (effect on the active amount of LDLR located on the surface of hepatic cells). In fact, recent results have indicated that peptide T9 (350 μM), when coincubated with GOF mutated PCSK9, restores the LDLR protein level by 74.3 ± 4.4%.[19] For this reason, T9D8A_1 reestablishes the LDLR protein level by 12.7% more than the parent T9.

In conclusion, the prediction of the binding free energy values of the alanine mutated T9 analogs suggested that the residues in positions 11, 13, and 14 can be considered hot spots of the PCSK9^{D374Y}/T9 interaction, considering that their mutation into alanine significantly weakened the binding free energy. At the end of this procedure, peptide T9D8A showed the highest estimated affinity compared to that predicted for the reference peptide T9. A further optimization of the structure, in order to design new and more potent PCSK9^{D374Y} inhibitors, was achieved by accomplishing additional mutations into the non-hot residues, replacing them by different natural amino acids. Applying the MM-GBSA approach and two steps of PRIME calculations, the T9 analog named T9D8A_1 was designed and synthesized. Experimental *in vitro* tests, as well as cellular assays, confirmed the success of the applied strategy to improve the biological activity of these peptides.

Based on these evidence, the T9D8A_1 analog possesses great potentiality for further structural optimization, being more biologically active than T9. We are aware that peptides are not usually considered highly bioavailable drugs; however, they are valuable biochemical tools and starting points for designing new small-molecules, such as peptidomimetics, active on the GOF PCSK9^{D374Y}.

DOI: 10.1021/acsmedchemlett.8b00464
ACS Med. Chem. Lett. 2019, 10, 425−430

EXPERIMENTAL PROCEDURES

PCSK9^{D374Y}/T9 Model and Peptide Binding Free Energy Estimation. The PCSK9^{D374Y} model were previously developed by us.[19] T9, as well as the new designed analogs, were charged on the N- and C-terminal ends. The rough PCSK9^{D374Y}/T9 model was optimized by energy minimization and 400 ns long MD simulations, by *pmemd.cuda* algorithm of Amber 2017 package.[20] Then, the acquired trajectory was examined by visual inspection with VMD,[27] ensuring that the thermalization did not cause any structural distortion. For additional details, see the experimental section of refs 5, 19, 25, and 26. MM-GBSA calculations were performed on the mutant PCSK9^{D374Y}/T9 complexes. The alanine mutants were built systematically altering the peptide sequence on the PCSK9^{D374Y}/T9 complex, by *tleap* module of Ambertools16.[20] The resulting complexes were energy minimized and equilibrated once more by MD simulations, adopting the procedure and the parameters previously applied.[5] In these cases, more than 100 ns of MD simulations were accomplished in the production runs, for each mutant complex. A hundred snapshots were regularly extracted from the trajectories to ensure the lowest standard error in the free energy estimation and the lowest calculation time. The time intervals for the extraction were chosen dividing by 100 the number of frames in which the systems showed the geometrical stability. MM-GBSA calculations were performed by *MM-PBSA.py* module[28] of Amber 2017 package,[20] keeping parameters in the default values. In these calculations, the single trajectory approach was applied, and the entropy contributions to the binding free energy, coming from the normal-mode analysis, was neglected. For this reason, the estimated binding free energy values are termed ΔG^*.

PRIME Calculations. Aiming to improve the affinity of T9D8A, a systematic mutation of the "non-hot" positions suggested by alanine scanning analysis were carried out. The "protein preparation wizard" module implemented in the Schrödinger suite for molecular modeling ensured the accuracy of the PCSK9^{D374Y}/T9D8A complex conformation equilibrated by MD simulations. In particular, the procedure permitted (1) to correctly assign the residue protonation state at pH 7.4, (2) to check the residue completeness, and (3) to eliminate atomic clashes. Then, 10,000 possible peptides were generated by mutations on the selected positions. The resulting complexes were minimized by Prime MM-GBSA, which uses OPLS3[29] as force field and a continuum solvent model to include the solvent effect into the calculations. Finally, affinity maturation functionality in BioLuminate (Prime MM-GBSA, Schrödinger, LLC, New York, NY, 2017) estimated the change in affinity ($\Delta\Delta G$) between PCSK9^{D374Y} and the generated peptides with respect to T9D8A.

Chemicals. All reagents and kits used for the biological characterization were purchased from commercial sources. More details are reported in the Supporting Information.

PCSK9^{D374Y}-LDLR PPI Evaluation. Peptides T9D8A and T9D8A_1 (0.1 μM to 1.0 mM) were investigated using the *in vitro* PCSK9-LDLR binding assay from CircuLex, following the conditions previously described.[19] More details are reported in the Supporting Information.

Cell Culture and Treatment Conditions. The HepG2 cell line was cultured following the procedure previously described.[30] The HepG2 cells (3×10^4/well) were starved overnight (ON), and then they were treated with 4.0 μg/mL PCSK9^{D374Y} and 10.0 μM T9D8A_1 in the presence of 4.0 μg/mL PCSK9^{D374Y} and vehicle (H_2O) for 2 h at 37 °C in the 5% CO_2 incubator.

Cell Fixation and In-Cell Western (ICW). Treated HepG2 cells were fixed in 4% paraformaldehyde for 20 min at room temperature (RT), and samples have been processed for ICW assay following the procedure described in the Supporting Information.

Fluorescent LDL Uptake Cell-Based Assay. The fluorescent LDL uptake cell-based assay was carried out using the procedure previously reported.[5] Additional details are reported in the Supporting Information.

Statistically Analysis. Statistical analyses were carried out by *t*-student (Graphpad Prism 6). Values were expressed as means ± SD; *p*-values < 0.05 were considered significant.

ASSOCIATED CONTENT

Supporting Information

The Supporting Information is available free of charge on the ACS Publications website at DOI: 10.1021/acsmedchemlett.8b00464.

Figures S1 and S2, Table S1, and additional experimental details (PDF)

AUTHOR INFORMATION

Corresponding Author

*E-mail: giovanni.grazioso@unimi.it. Phone: +39-0250319352. Fax: +39-0250319359.

ORCID

Carmen Lammi: 0000-0002-7428-4486
Jacopo Sgrignani: 0000-0002-8633-1032
Anna Arnoldi: 0000-0002-0987-3014
Giovanni Grazioso: 0000-0002-3261-9356

Author Contributions

The manuscript was written through contributions of all authors. All authors have given approval to the final version of the manuscript.

Funding

This research was supported by the Fondazione Banca del Monte di Lombardia (PV).

Notes

The authors declare no competing financial interest.

ACKNOWLEDGMENTS

G.G. acknowledges the CINECA and the "Regione Lombardia" award under the LISA initiative, for the availability of high performance computing resources and support. We are indebted to Carlo Sirtori Foundation (Milan, Italy) for having provided part of the equipment used in this experimentation.

REFERENCES

(1) Cunningham, D.; Danley, D. E.; Geoghegan, K. F.; Griffor, M. C.; Hawkins, J. L.; Subashi, T. A.; Varghese, A. H.; Ammirati, M. J.; Culp, J. S.; Hoth, L. R.; Mansour, M. N.; McGrath, K. M.; Seddon, A. P.; Shenolikar, S.; Stutzman-Engwall, K. J.; Warren, L. C.; Xia, D.; Qiu, X. Structural and biophysical studies of PCSK9 and its mutants linked to familial hypercholesterolemia. *Nat. Struct. Mol. Biol.* **2007**, *14*, 413.

(2) Horton, J. D.; Cohen, J. C.; Hobbs, H. H. Molecular biology of PCSK9: its role in LDL metabolism. *Trends Biochem. Sci.* **2007**, *32*, 71−7.

(3) Everett, B. M.; Smith, R. J.; Hiatt, W. R. Reducing LDL with PCSK9 Inhibitors−The Clinical Benefit of Lipid Drugs. *N. Engl. J. Med.* **2015**, *373*, 1588−91.

(4) Gustafsen, C.; Olsen, D.; Vilstrup, J.; Lund, S.; Reinhardt, A.; Wellner, N.; Larsen, T.; Andersen, C. B. F.; Weyer, K.; Li, J.-p.; Seeberger, P. H.; Thirup, S.; Madsen, P.; Glerup, S. Heparan sulfate proteoglycans present PCSK9 to the LDL receptor. *Nat. Commun.* **2017**, *8*, 503.

(5) Lammi, C.; Zanoni, C.; Aiello, G.; Arnoldi, A.; Grazioso, G. Lupin peptides modulate the protein-protein interaction of PCSK9 with the low density lipoprotein receptor in HepG2 cells. *Sci. Rep.* **2016**, *6*, 29931.

(6) Stucchi, M.; Grazioso, G.; Lammi, C.; Manara, S.; Zanoni, C.; Arnoldi, A.; Lesma, G.; Silvani, A. Disrupting the PCSK9/LDLR

DOI: 10.1021/acsmedchemlett.8b00464
ACS Med. Chem. Lett. 2019, 10, 425−430

protein-protein interaction by an imidazole-based minimalist peptidomimetic. *Org. Biomol. Chem.* **2016**, *14*, 9736−9740.
(7) Zhang, Y.; Eigenbrot, C.; Zhou, L.; Shia, S.; Li, W.; Quan, C.; Tom, J.; Moran, P.; Di Lello, P.; Skelton, N. J.; Kong-Beltran, M.; Peterson, A.; Kirchhofer, D. Identification of a small peptide that inhibits PCSK9 protein binding to the low density lipoprotein receptor. *J. Biol. Chem.* **2014**, *289*, 942−55.
(8) Dong, B.; Li, H.; Singh, A. B.; Cao, A.; Liu, J. Inhibition of PCSK9 transcription by berberine involves down-regulation of hepatic HNF1α protein expression through the ubiquitin-proteasome degradation pathway. *J. Biol. Chem.* **2015**, *290*, 4047−58.
(9) Salmaso, V.; Sturlese, M.; Cuzzolin, A.; Moro, S. Exploring Protein-Peptide Recognition Pathways Using a Supervised Molecular Dynamics Approach. *Structure* **2017**, *25*, 655−662.e2.
(10) Ahrens, V. M.; Bellmann-Sickert, K.; Beck-Sickinger, A. G. Peptides and peptide conjugates: therapeutics on the upward path. *Future Med. Chem.* **2012**, *4*, 1567−86.
(11) Fosgerau, K.; Hoffmann, T. Peptide therapeutics: current status and future directions. *Drug Discovery Today* **2015**, *20*, 122−8.
(12) Shan, L.; Pang, L.; Zhang, R.; Murgolo, N. J.; Lan, H.; Hedrick, J. A. PCSK9 binds to multiple receptors and can be functionally inhibited by an EGF-A peptide. *Biochem. Biophys. Res. Commun.* **2008**, *375*, 69−73.
(13) Lammi, C.; Zanoni, C.; Calabresi, L.; Arnoldi, A. Lupin protein exerts cholesterol-lowering effects targeting PCSK9: from clinical evidences to elucidation of the *in vitro* molecular mechanism using HepG2 cells. *J. Funct. Foods* **2016**, *23*, 230−240.
(14) Zanoni, C.; Aiello, G.; Arnoldi, A.; Lammi, C. Investigations on the hypocholesterolaemic activity of LILPKHSDAD and LTFPGSAED, two peptides from lupin beta-conglutin: Focus on LDLR and PCSK9 pathways. *J. Funct. Foods* **2017**, *32*, 1−8.
(15) Zhang, Y.; Ultsch, M.; Skelton, N. J.; Burdick, D. J.; Beresini, M. H.; Li, W.; Kong-Beltran, M.; Peterson, A.; Quinn, J.; Chiu, C.; Wu, Y.; Shia, S.; Moran, P.; Di Lello, P.; Eigenbrot, C.; Kirchhofer, D. Discovery of a cryptic peptide-binding site on PCSK9 and design of antagonists. *Nat. Struct. Mol. Biol.* **2017**, *24*, 848−856.
(16) Naoumova, R. P.; Tosi, I.; Patel, D.; Neuwirth, C.; Horswell, S. D.; Marais, A. D.; van Heyningen, C.; Soutar, A. K. Severe hypercholesterolemia in four British families with the D374Y mutation in the PCSK9 gene: long-term follow-up and treatment response. *Arterioscler., Thromb., Vasc. Biol.* **2005**, *25*, 2654−60.
(17) Bottomley, M. J.; Cirillo, A.; Orsatti, L.; Ruggeri, L.; Fisher, T. S.; Santoro, J. C.; Cummings, R. T.; Cubbon, R. M.; Lo Surdo, P.; Calzetta, A.; Noto, A.; Baysarowich, J.; Mattu, M.; Talamo, F.; De Francesco, R.; Sparrow, C. P.; Sitlani, A.; Carfi, A. Structural and biochemical characterization of the wild type PCSK9-EGF(AB) complex and natural familial hypercholesterolemia mutants. *J. Biol. Chem.* **2009**, *284*, 1313−23.
(18) Lagace, T. A.; Curtis, D. E.; Garuti, R.; McNutt, M. C.; Park, S. W.; Prather, H. B. Secreted PCSK9 decreases the number of LDL receptors in hepatocytes and inlivers of parabiotic mice. *J. Clin. Invest.* **2006**, *116*, 2995.
(19) Grazioso, G.; Bollati, C.; Sgrignani, J.; Arnoldi, A.; Lammi, C. The first food-derived peptide inhibitor of the protein-protein interaction between Gain-of-Function PCSK9^{D374Y} and the LDL receptor. *J. Agric. Food Chem.* **2018**, *66*, 10552−10557.
(20) Case, D. A.; Cerutti, D. S.; Cheatham, T.E., III; Darden, T. A.; Duke, R. E.; Giese, T. J.; Gohlke, H.; Goetz, A. W.; Greene, D.; Homeyer, N.; Izadi, S.; Kovalenko, A.; Lee, T. S.; LeGrand, S.; Li, P.; Liu, J.; Luchko, T.; Luo, R.; Mermelstein, D.; Merz, K. M.; Monard, G.; Nguyen, H.; Omelyan, I.; Onufriev, A.; Pan, F.; Qi, R.; Roe, D. R.; Roitberg, A.; Sagui, C.; Simmerling, C. L.; Botello-Smith, W. M.; Swails, J.; Walker, R. C.; Wang, J.; Wolf, R. M.; Wu, X.; Xiao, L.; York, D. M.; Kollman, P. A. *AMBER 2017*; University of California: San Francisco, 2017.
(21) Moreira, I. S.; Fernandes, P. A.; Ramos, M. J. Unraveling the importance of protein-protein interaction: application of a computational alanine-scanning mutagenesis to the study of the IgG1 streptococcal protein G (C2 fragment) complex. *J. Phys. Chem. B* **2006**, *110*, 10962−9.
(22) Homeyer, N.; Stoll, F.; Hillisch, A.; Gohlke, H. Binding Free Energy Calculations for Lead Optimization: Assessment of Their Accuracy in an Industrial Drug Design Context. *J. Chem. Theory Comput.* **2014**, *10*, 3331−3344.
(23) Lammi, C.; Aiello, G.; Vistoli, G.; Zanoni, C.; Arnoldi, A.; Sambuy, Y.; Ferruzza, S.; Ranaldi, G. A multidisciplinary investigation on the bioavailability and activity of peptides from lupin protein. *J. Funct. Foods* **2016**, *24*, 297−306.
(24) Lammi, C.; Zanoni, C.; Arnoldi, A. A simple and high-throughput in-cell Western assay using HepG2 cell line for investigating the potential hypocholesterolemic effects of food components and nutraceutics. *Food Chem.* **2015**, *169*, 59−64.
(25) Catto, C.; Grazioso, G.; Dell'Orto, S.; Gelain, A.; Villa, S.; Marzano, V.; Vitali, A.; Villa, F.; Cappitelli, F.; Forlani, F. The response of Escherichia coli biofilm to salicylic acid. *Biofouling* **2017**, *33*, 235−251.
(26) Villa, S.; Legnani, L.; Colombo, D.; Gelain, A.; Lammi, C.; Bongiorno, D.; Ilboudo, D. P.; McGee, K. E.; Bosch, J.; Grazioso, G. Structure-based drug design, synthesis and biological assays of P. falciparum Atg3-Atg8 protein-protein interaction inhibitors. *J. Comput.-Aided Mol. Des.* **2018**, *32*, 473−486.
(27) Humphrey, W.; Dalke, A.; Schulten, K. VMD: visual molecular dynamics. *J. Mol. Graphics* **1996**, *14*, 33−38.
(28) Miller, B. M., III; McGee, T. D., Jr.; Swails, J. M.; Homeyer, N.; Gohlke, H.; Roitberg, A. E. MMPBSA.py: An Efficient Program for End-State Free Energy Calculations. *J. Chem. Theory Comput.* **2012**, *8*, 3314−3321.
(29) Beard, H.; Cholleti, A.; Pearlman, D.; Sherman, W.; Loving, K. A. Applying physics-based scoring to calculate free energies of binding for single amino acid mutations in protein-protein complexes. *PLoS One* **2013**, *8*, e82849.
(30) Lammi, C.; Zanoni, C.; Scigliuolo, G. M.; D'Amato, A.; Arnoldi, A. Lupin peptides lower low-density lipoprotein (LDL) cholesterol through an up-regulation of the LDL receptor/sterol regulatory element binding protein 2 (SREBP2) pathway at HepG2 cell line. *J. Agric. Food Chem.* **2014**, *62*, 7151−9.

DOI: 10.1021/acsmedchemlett.8b00464
ACS Med. Chem. Lett. 2019, 10, 425−430